DEVELOPING REGIONALIZED MODELS OF LITHOSPHERIC THICKNESS AND VELOCITY STRUCTURE ACROSS EURASIA AND THE MIDDLE EAST FROM JOINTLY INVERTING P-WAVE AND S-WAVE RECEIVER FUNCTIONS WITH RAYLEIGH WAVE GROUP AND PHASE VELOCITIES

Jordi Julià[1], Andrew A. Nyblade[1], Samantha E. Hansen[1], Arthur J. Rodgers[2], and Eric Matzel[2]

Penn State University[1] and Lawrence Livermore National Laboratory[2]

Sponsored by the National Nuclear Security Administration

Award Nos. DE-AC52-09NA29322[1] and DE-AC52-07NA27344[2]
Proposal No. BAA09-13

ABSTRACT

In this project, we are developing models of lithospheric structure for a wide variety of tectonic regions throughout Eurasia and the Middle East by regionalizing 1D velocity models obtained by jointly inverting *P*-wave and *S*-wave receiver functions with Rayleigh wave group and phase velocities. We expect the regionalized velocity models will improve our ability to predict travel-times for local and regional phases, such as Pg, Pn, Sn and Lg, as well as travel-times for body-waves at upper mantle triplication distances in both seismic and aseismic regions of Eurasia and the Middle East. We anticipate the models will help inform and strengthen ongoing and future efforts within the NNSA labs to develop 3D velocity models for Eurasia and the Middle East, and will assist in obtaining model-based predictions where no empirical data are available and for improving locations from sparse networks using kriging.

The codes needed to conduct the joint inversion of *P*-wave receiver functions (PRFs), *S*-wave receiver functions (SRFs), and dispersion velocities have already been assembled as part of ongoing research on lithospheric structure in Africa. The methodology has been tested with synthetic "data" and case studies have been investigated with data collected at an open broadband station in South Africa. PRFs constrain the size and *S*-*P* travel-time of seismic discontinuities in the crust and uppermost mantle, SRFs constrain the size and *P*-*S* travel-time of the lithosphere-sublithosphere boundary, and dispersion velocities constrain average *S*-wave velocity within frequency-dependent depth-ranges. Preliminary results show that the combination yields integrated 1D velocity models local to the recording station, where the discontinuities constrained by the receiver functions are superimposed to a background velocity model constrained by the dispersion velocities.

In our first year of this project we will (i) generate 1D velocity models for open broadband seismic stations in the western half of the study area (Eurasia and the Middle East) and (ii) identify well located seismic events with event-station paths isolated to individual tectonic provinces within the study area and collect broadband waveforms and source parameters for the selected events. The 1D models obtained from the joint inversion will then be combined with published geologic terrain maps to produce regionalized models for distinctive tectonic areas within the study area, and the models will be validated through full waveform modeling of well-located seismic events recorded at local and regional distances.

OBJECTIVES

Velocity models of lithospheric structure (crust and uppermost mantle) are critical for accurately predicting travel times and the propagation of local and regional seismic phases, such as Pg, Pn, Sn and Lg. The stability of wave propagation for these and other phases of relevance to improving our capability to locate and discriminate seismic events can be greatly affected by 2- and 3-D heterogeneity in both lithospheric and sublithospheric structure. In particular, velocity models of the lithosphere are key to accurately modeling travel times, in addition to surface wave dispersion and full waveforms at regional (2^o-15^o) and far-regional (15^o-25^o) distances.

Ongoing efforts within the National Nuclear Security Administration (NNSA) labs to develop 3-D velocity models for Eurasia and the Middle East are the Seismic Location Baseline Model (SLBM) and its follow-on, the Regional Seismic Travel Time project (RSTT). Starting models for SLBM inversions include the WENA model (Pasyanos et al., 2004) and the UNIFIED model (Pasyanos et al., 2003), which have been constructed from *a priori* information in the published literature. These models subdivide Eurasia and the Middle East into tectonically distinct regions, as shown in Figure 1, each of which is characterized by multiple sediment, crustal, and upper mantle layers with specified thicknesses, compressional and shear velocities, densities, and attenuation factors (Pasyanos et al., 2004). However, below the Moho, the models consist of a mantle half-space with a constant velocity gradient. As such, the SLBM inversions cannot accurately model rays penetrating below the lithosphere and cannot be used for waveform modeling or travel time predictions past about 12°.

The main objective of this project is to develop new velocity models of lithospheric thickness and velocity structure for Eurasia and the Middle East with predictive capabilities past 12^o. To develop such models, local velocity models will be first obtained by jointly inverting multiple datasets collected at open broadband stations, including *P*-wave receiver functions (PRFs), *S*-wave receiver functions (SRFs), fundamental-mode Rayleigh-wave phase velocities, and fundamental-mode Rayleigh-wave group velocities. The local 1D models will then be combined for stations within tectonic regions identified in the WENA and UNIFIED models to produce regionalized velocity models of the crust and upper mantle. These regionalized, 1-D models will characterize the average structure within the corresponding tectonic region, including lithospheric thickness, velocity structure of the lithospheric mantle, and structure of the low-velocity zone beneath the lithospheric lid, and have better resolution than other published

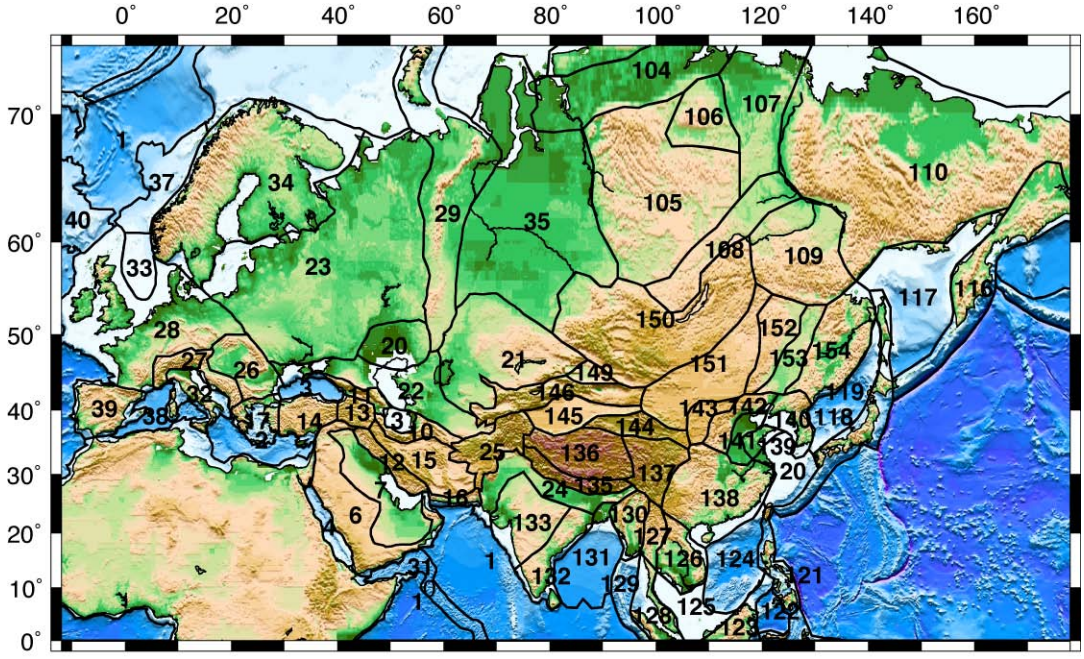

Figure 1. The UNIFIED model, with contributions from both LLNL and LANL. The numbered areas mark tectonically distinct regions defined by Pasyanos et al. (2003; 2004).

models for Eurasia and the Middle East as they will be fitting four independent seismic datasets. Moreover, a large number of seismic stations are openly available across Eurasia and the Middle East, which allows average 1-D models to be obtained for the majority of tectonic regions identified in the WENA and UNIFIED models.

The regionalized models will be evaluated with 1-D waveform modeling for events with well-determined source parameters (depth, seismic moment, and focal mechanism) and broadband recordings with ray-paths predominately in a single tectonic/geologic region. The model validation efforts will focus on regions where there is good event-station coverage (i.e., pure path propagation with a region) over a range of local and regional distances and will also include an investigation of the misfits between data and synthetics to understand how the regionalized models need to be perturbed to improve the fits in phase and amplitude.

The regionalized velocity models will improve our ability to predict Pg, Pn, Sn and Lg travel times in both seismic and aseismic regions of Eurasia and the Middle East and will help inform and strengthen ongoing and future efforts within the NNSA labs to develop 3-D velocity models for Eurasia and the Middle East. Importantly, our new velocity models will assist in obtaining model-based predictions where no empirical data are available (e.g., Flanagan et al., 2006), and in improving locations from sparse networks (e.g., Schultz et al., 1998; Myers and Schultz, 2000).

RESEARCH ACCOMPLISHED

The deliverables for the first year of application of this project include the development of joint inversion models for the western half of the study area. The development of the joint inversion codes needed to conduct the proposed research was already completed as part of an investigation of the lithospheric structure of southern Africa. We have now started gathering the data needed for the application of the joint inversion procedure.

Data Gathering

PRF and SRF waveforms for Eurasia and the Middle East will be obtained for all of the broadband stations belonging to the open networks available through the Incorporated Research Institutions for Seismology (IRIS) Data Management Center, both permanent and temporary. For the western half of the study area (Europe and the Middle East), the number of available stations totals 273 and have recording time windows ranging from a few years (e.g., station ROGR, belonging to the temporary RUSH deployment in Scotland) to almost two decades (e.g., station OBN, in Russia, which is part of the permanent GSN network).

Seismic sources ideally suited for the computation of PRFs commonly are at epicentral distances between 30^{o} and 90^{o} from the recording station and have magnitudes above 5.5. Following these criteria a total of 4,713 seismic sources have been selected from the Weekly Hypocenter Data File catalog, and the corresponding waveforms have already been downloaded for all the selected stations. The events have been recorded in the hundreds for the stations with the shorter recording time windows and in the thousands for the stations with the longer recording time windows. PRFs are presently being computed. The selection criteria for seismic sources commonly considered for the computation of SRFs are considerably more restrictive due to the interference of other teleseismic waves with the time window of interest, and include epicentral distances between 60^{o} and 85^{o} and magnitudes above 5.7 (see Wilson et al., 2006). The waveforms for the computation of SRFs at the selected stations are being downloaded.

Rayleigh wave group and phase velocities across Eurasia and the Middle East, on the other hand, will be obtained from a number of independent surface-wave tomography studies. Group velocity studies include Ritzwoller and Levshin (1998), who generated Rayleigh wave group velocity maps from 20 to 200 s with a resolution of about 5^{o} across most of Eurasia using about 9000 dispersion measurements, and Pasyanos (2005), who measured over 30,000 Rayleigh wave dispersion curves and used the conjugate gradient method with variable smoothness to invert for surface wave group velocity across Eurasia, the Middle East and surrounding areas. The Pasyanos (2005) model highlights lateral variations across the region for periods between 7 and 100 s with a resolution approaching 1^{o}. Phase velocities studies include those of Ekström et al. (1997), who used a method based on phase-matched filter theory to develop a global surface wave phase velocity model for periods between 35 and 150 s and, on a more regional scale, Curtis et al. (1998) who obtained phase velocity measurements along 4,020 Rayleigh wave paths across Eurasia and inverted this data for phase velocity maps at periods between 26 and 150 s. Overall, excellent coverage across Eurasia and the Middle East is provided by these studies, extending from periods of approximately

5 to 150 s, providing sensitivity within the crust as well as down into the lithospheric and sublithospheric mantle.

Code Development

The joint inversion of PRFs, SRFs, and surface-wave dispersion velocities is a straight-forward extension of the iterative, linearized scheme introduced by Julià et al. (2000; 2003) to jointly invert PRFs and dispersion velocities. The joint inversion scheme integrates the constraints conveyed by the individual datasets into velocity models that simultaneously explain all the data sets. PRFs constrain *S*-wave velocity contrasts across discontinuities and vertical *S*-*P* travel-times, but do not uniquely constrain the subsurface structure (Ammon et al., 1990); surface-wave dispersion velocities constrain absolute *S*-wave velocities within broad, frequency-dependent depth-ranges, but do not resolve rapid velocity variations with depth. Both data sets are thus sensitive to the same parameter, *S*-wave velocity, and the constraints complement each other, so that they bridge resolution gaps between the datasets. The combination produces *S*-wave velocity models where the high-resolution details constrained by the receiver functions are superimposed to a background velocity model constrained by the dispersion velocities (Julià et al., 2000). The joint inversion scheme has been applied to a variety of tectonic settings around the world, which include the Arabian shield (Julià et al., 2003), East Africa (Julià et al., 2005; Dugda et al., 2007; Keranen et al., 2009), the Paraná basin of Brazil (Julià et al., 2008), and the Indian shield (Julià et al., 2009).

The joint inversion scheme of Julià et al. (2000; 2003) is implemented through the following set of equations:

$$\begin{bmatrix} \sqrt{\frac{p}{w_s^2}}\, D_s \\ \sqrt{\frac{q}{w_b^2}}\, D_b \\ \sigma\Delta \\ A \end{bmatrix} \vec{m} = \begin{bmatrix} \sqrt{\frac{p}{w_s^2}}\, \vec{r}_s \\ \sqrt{\frac{q}{w_b^2}}\, \vec{r}_b \\ \vec{0} \\ A\,\vec{m}_a \end{bmatrix} + \begin{bmatrix} \sqrt{\frac{p}{w_s^2}}\, D_s \\ \sqrt{\frac{q}{w_b^2}}\, D_b \\ \vec{0} \\ \vec{0} \end{bmatrix} \vec{m}_o \qquad (1)$$

where D_s and D_b are partial derivative matrices for the dispersion and the PRF estimates, respectively, $\mathbf{r}_s$ and $\mathbf{r}_b$ are the corresponding vectors of residuals, w_s^2 and w_b^2 are weights that equalize the data sets, the vector **m** contains the velocities of fixed thickness layers overlying a half-space, and $\mathbf{m}_0$ contains an initial estimate for the velocities. The matrix Δ constructs the second difference model and makes the resulting profiles vary smoothly, and the diagonal matrix W contains constraint weights to the *a priori* velocity values $\mathbf{m}_a$. The influence factor 'p' controls the trade-off between fitting the receiver functions and the dispersion curves, and the smoothness parameter σ controls the trade-off between fitting the data and model smoothness. The values of these parameters are determined empirically by performing suites of inversions. The parameter q=1-p, with $0 \leq p \leq 1$, so that p = 0 means inverting receiver function data only and p = 1 means inverting dispersion data only. The weights w_s^2 and w_b^2 are computed as $N\sigma^2$, where N is the number of data points and σ^2 is the variance of the observations.

SRFs have been incorporated into the joint inversion scheme by simply adding the partial derivatives and the vector of residuals into D_b and $\mathbf{r}_b$, respectively, in the system of equations (1). Similar to PRFs, SRFs constrain *S*-wave velocity contrasts across seismic discontinuities and vertical P-S travel-times, but do not uniquely constrain the subsurface structure. The main contribution is that SRFs provide better constraints on the depth and structure of the lithosphere-asthenosphere boundary than PRFs (e.g., Kumar et al., 2007; Hansen et al., 2007) and that they help reduce trade-offs within the upper mantle. The performance of the new methodology is illustrated through inversion of noise-free, "synthetic" data in Figure 2. The starting model is a simple half-space of ~4.0 km/s, parameterized as a stack of thin layers of constant velocity and thickness. After the first iteration the match between "observed" and predicted dispersion velocities improves dramatically, and this translates into an inverted model with average velocities close to that of the true model. The predicted receiver functions, however, do not match the peaks and troughs correctly, and the discontinuities are shifted in the inverted model with respect to the true model. After the second iteration the match between "observed" and predicted receiver functions improves, and the depths of the discontinuities are placed at the expected depths. Subsequent iterations keep tuning the inverted models until a perfect match to the true model is achieved.

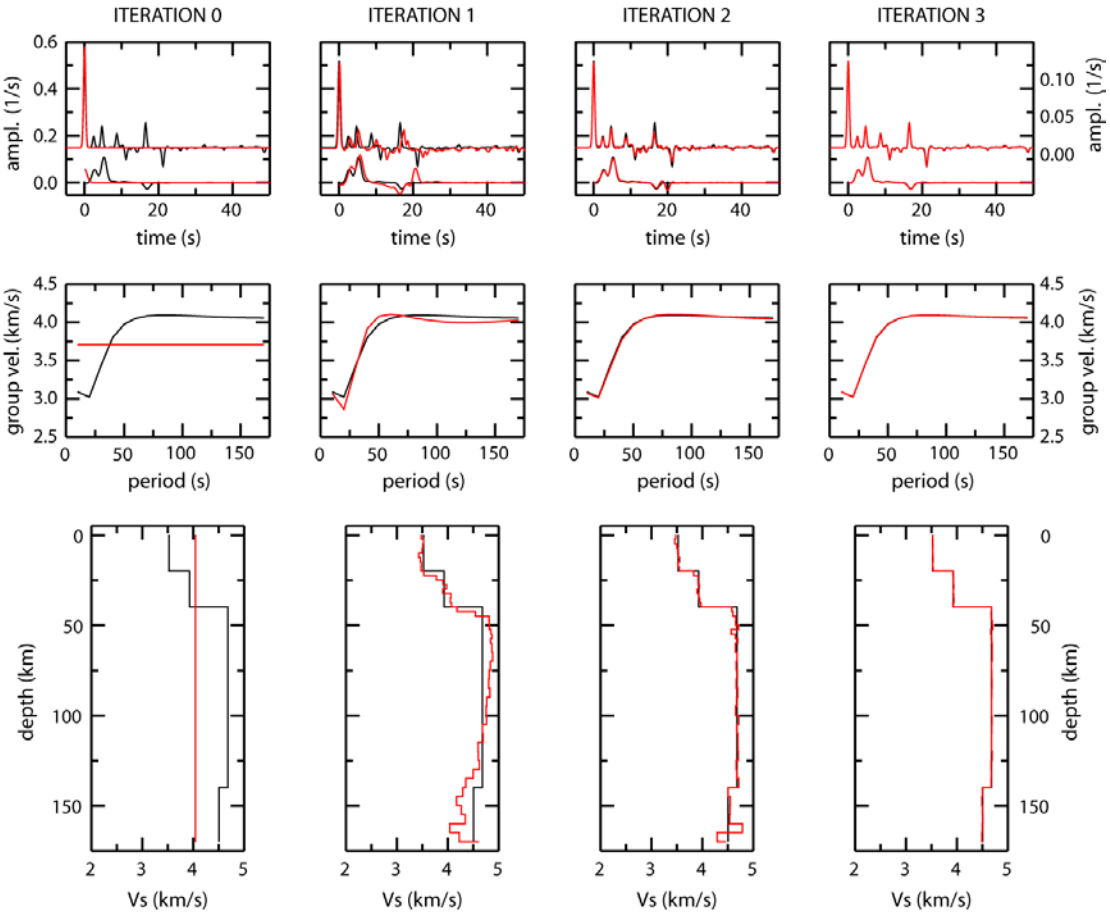

Figure 2. Joint inversion of synthetic PRFs, SRFs, and dispersion velocities. Each columns displays the joint inversion after each iteration (indicated on top). The top frames display "observed" (black) and predicted (red) PRF (upper trace) and SRF (lower trace) waveforms; the middle frames show the "observed" (black) and predicted (red) Rayleigh-wave group velocities; and the bottom frames show the inverted (red) and true (black) velocity models.

Figure 3 shows the results of jointly inverting PRFs, SRFs, and surface-wave dispersion velocities at station BOSA, which is located in the stable interior of the Kaapvaal craton in southern Africa. The figure shows 6 PRF averages (4 of them at two overlapping frequency bands) obtained by stacking the receiver functions for this station in tight ray parameter and back-azimuth ranges, 1 SRF average, and fundamental-mode Rayleigh wave dispersion velocities obtained from the tomographic inversion of Pasyanos (2005). The starting model was constructed as a 40-km thick gradational crust overlying PREM (Dziewonski and Anderson, 1981). Note that a single model can satisfactorily match all the PRF and SRF averages, implying that the structure under the station is laterally homogeneous, as well as the dispersion velocities. In the inverted model, the crust is ~35 km thick and is separated from the uppermost mantle by a sharp discontinuity, which is in excellent agreement with independent seismic studies (e.g., Niu and James, 2002). The upper mantle consists of a linear velocity increase down to ~160 km depth, a small LVZ between 160 and 180 km depth, and a velocity decrease at ~240 km depth. Figure 3 also overlays the velocity model resulting from the joint inversion of PRFs and dispersion velocities only. Little difference is observed down to ~150 km depth between the joint inversion models with and without the SRF. The main differences lie in the sublithospheric mantle where the small LVZ between 160 and 180 km depth and the velocity decrease at ~240 km depth are required to match the SRF waveforms. The overlay demonstrates that the upper mantle features are mainly constrained by the SRF waveforms, as the velocities are averaged through a linear velocity increase down to ~270 km in the joint inversion models with no SRF constraints.

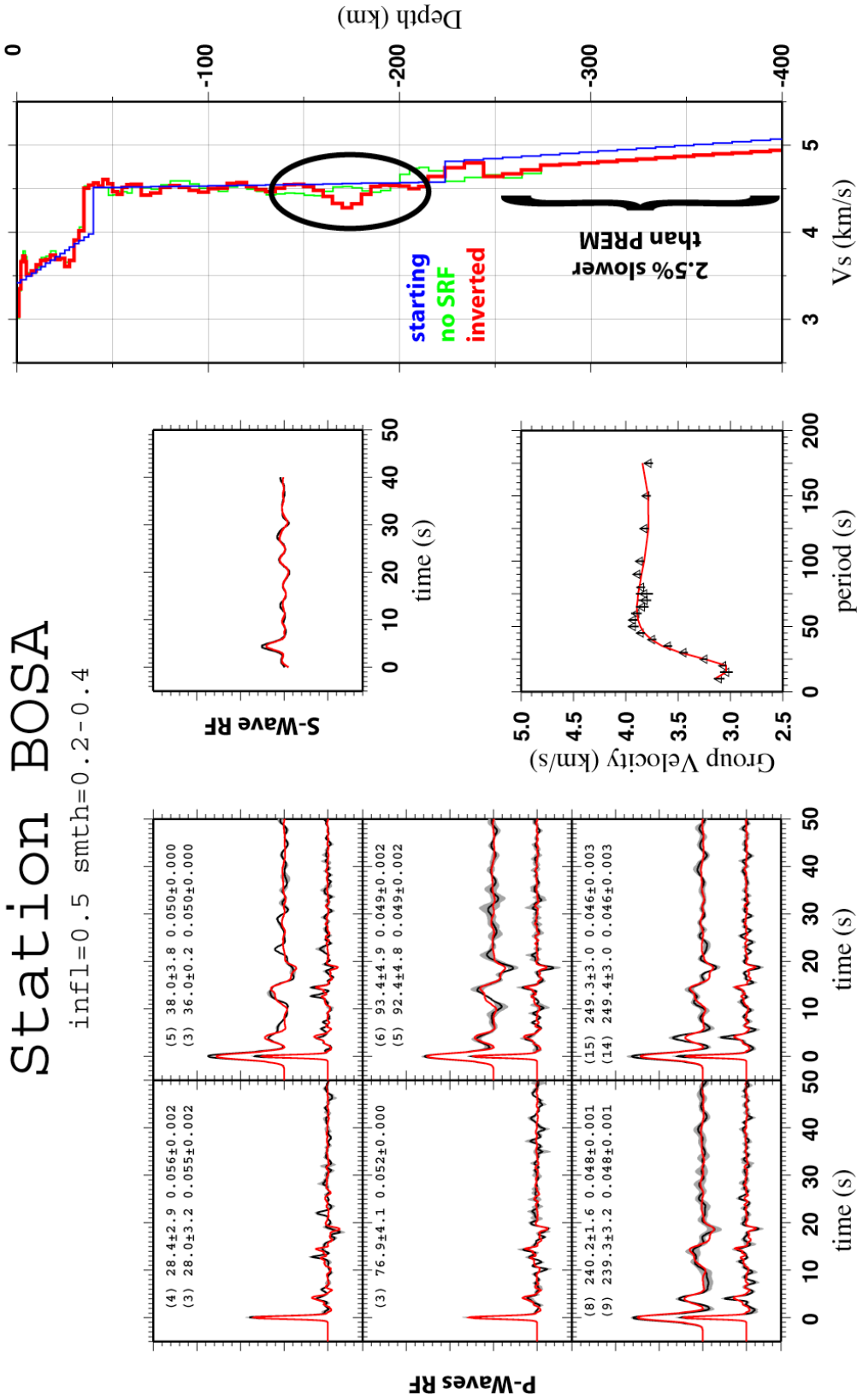

Figure 3. Joint inversion results at station BOSA in southern Africa. The left panels display the six PRF averages (black) and the corresponding predictions (red) from the joint inversion model. The middle panels show the SRF averages (black) and the corresponding prediction (red) in the top and the observed (triangles) and predicted (red line) dispersion velocities at the bottom. The right panel overlays the starting (blue), and inverted models with (red) and without (green) SRF constraints.

CONCLUSIONS AND RECOMMENDATIONS

We have started downloading broadband seismic waveforms needed for the computation of PRFs and SRFs from the seismic stations within western Eurasia and the Middle East that are openly available through the IRIS archive. The resulting dataset consists of tens of thousands of waveforms recorded in as many as 273 broadband stations. The codes needed to jointly invert the complementary seismic data sets have already been implemented and tested with broadband stations in southern Africa. The development of the joint inversion models for the targeted area will start as soon as the phase and group velocities are extracted from the corresponding tomographic studies and the computation of PRFs and SRFs is completed.

REFERENCES

Ammon, C., G. Randall, and G. Zandt (1990). On the nonuniqueness of receiver function inversions, *J. Geophys. Res.* 95: 15303–15318.

Curtis, A., J. Trampert, R. Snieder, and B. Dost (1998). Eurasian fundamental mode surface wave phase velocities and their relationship with tectonic structures, *J. Geophys. Res.* 103: 26919–26947.

Dugda, M., A. Nyblade, and J. Julià (2007). Thin lithosphere beneath the Ethiopian Plateau revealed by a joint inversion of Rayleigh wave group velocities and receiver functions, *J. Geophys. Res.* 112: doi: 10.1029/2006JB004918.

Dziewonski, A., and D. Anderson (1981). Preliminary reference earth model, *Phys. Earth Plant. Int.* 25: 297–356.

Ekström, G., J. Tromp, and E. Larson (1997). Measurements and global models of surface wave propagation, *J. Geophys. Res.* 102: 8137–8157.

Flanagan, M., S. Myers, and K. Koper (2006). Regional travel-time uncertainty and seismic location improvement using a three-dimensional a priori velocity model, *EOS Trans. AGU* 87: S31B-0194.

Hansen, S., A. Rodgers, S. Schwartz, and A. Al-Amri (2007). Imaging ruptured lithosphere beneath the Red Sea and Arabian Peninsula, *Earth Planet. Sci. Lett.* 259: 256–265.

Julià, J., C. Ammon, R. Herrmann, and A.M. Correig (2000). Joint inversion of receiver function and surface wave dispersion observations, *Geophys. J. Int.* 143: 99–112.

Julià, J., C. Ammon, and R. Herrmann (2003). Lithospheric structure of the Arabian Shield from the joint inversion of receiver functions and surface-wave group velocities, *Tectonophysics* 371:1–21.

Julià, J., C. Ammon, and A. Nyblade (2005). Evidence for mafic lower crust in Tanzania, East Africa, from joint inversion of receiver functions and Rayleigh wave dispersion velocities, *Geophys. J. Int.* 162: 555–569.

Julià, J., M. Assumpção, and M. Rocha (2008). Deep crustal structure of the Paraná Basin from receiver functions and Rayleigh-wave dispersion: Evidence for a fragmented cratonic root, *J. Geophys. Res.* 113: B08318, doi:10.1029/2007jb005374.

Julià, J., J. Jagadeesh, S.S. Rai, and T.J. Owens (2009). Deep crustal structure of the Indian shield from joint inversion of P-wave receiver functions and Rayleigh-wave group velocities: Implications for Precambrian crustal evolution, *J. Geophys. Res.* (in press).

Keranen, K. M., S. L. Klemperer, J. Julia, J. F. Lawrence, and A. A. Nyblade (2009). Low lower crustal velocity across Ethiopia: Is the Main Ethiopian Rift a narrow rift in a hot craton?, *Geochem. Geophys. Geosyst.* 10: Q0AB01, doi:10.1029/2008GC002293.

Kumar, P., X.H. Yuan, M.R. Kumar, R. Kind, X.Q. Li, and R.K. Chadha (2007). The rapid drift of the Indian tectonic plate, *Nature* 449: 894–897.

Myers, S., and C. Schultz (2000). Improving sparse network seismic location with Bayesian kriging and teleseismically constrained calibration events, *Bull. Seis. Soc. Am.* 90: 199–211.

Niu, F., and D. James (2002), Fine structure of the lowermost crust beneath the Kaapvaal craton and its implications for crustal formation and evolution, *Earth Planet. Sci. Lett.* 200: 121–130.

Pasyanos, M., W. Walter, and M. Flanagan (2003). Geophysical models for nuclear explosion monitoring, in *Proceedings of the 25th Seismic Research Review—Nuclear Explosion Monitoring: Building the Knowledge Base*, LA-UR-03-6029, Vol. 1, pp. 125–134.

Pasyanos, M., W. Walter, M. Flanagan, P. Goldstein, and J. Bhattacharyya (2004). Building and testing an a priori geophysical model for western Eurasia and North America, *Pure Appl. Geophys* 161: 235–281.

Pasyanos, M. (2005). A variable resolution surface wave dispersion study of Eurasia, North Africa, and surrounding regions, *J. Geophys. Res.* 110: doi: 10.1029/2005JB003749.

Ritzwoller, M. and A. Levshin (1998). Eurasian surface wave tomography: group velocities, *J. Geophys. Res.* 103: 4839–4878.

Schultz, C., S. Myers, J. Hipp, and C. Young (1998). Nonstationary Bayesian kriging; a predictive technique to genereate spatial corrections for seismic detection, location, and identification, *Bull. Seis. Soc. Am.* 88: 1275–1288.

Wilson, D. C., D. A. Angus, J. F. Ni, and S. P. Grand (2006). Constraints on the interpretation of S-to-P receiver functions, *Geophys. J. Int.* 165: 969–980.